Molecular and Cellular Neuroscience **18,** 149–167 (2001)
doi:10.1006/mcne.2001.1012, *available online at http://www.idealibrary.com on* IDEAL®

MCN

The Dynamics of SAP90/PSD-95 Recruitment to New Synaptic Junctions

Tal Bresler, Yaron Ramati, Pedro L. Zamorano,* Rong Zhai,* Craig C. Garner,* and Noam E. Ziv

*Rappaport Institute and the Department of Anatomy and Cell Biology, Bruce Rappaport Faculty of Medicine, Technion, Haifa, Israel; and *Department of Neurobiology, The University of Alabama at Birmingham, Birmingham, Alabama*

SAP90/PSD-95 is thought to be a central organizer of the glutamatergic synapse postsynaptic reception apparatus. To assess its potential role during glutamatergic synapse formation, we used GFP-tagged SAP90/PSD-95, time lapse confocal microscopy, and cultured hippocampal neurons to determine its dynamic recruitment into new synaptic junctions. We report that new SAP90/PSD-95 clusters first appeared at new axodendritic contact sites within 20–60 min of contact establishment. SAP90/PSD-95 clustering was rapid, with kinetics that fit a single exponential with a mean time constant of ~23 min. Most new SAP90/PSD-95 clusters were found juxtaposed to functional presynaptic boutons as determined by labeling with FM 4–64. No evidence was found for the existence of discrete transport particles similar to those previously reported to mediate presynaptic active zone cytoskeleton assembly. Instead, we found that SAP90/PSD-95 is recruited to nascent synapses from a diffuse dendritic cytoplasmic pool. Our findings show that SAP90/PSD-95 is recruited to nascent synaptic junctions early during the assembly process and indicate that its assimilation is fundamentally different from that of presynaptic active zone components.

INTRODUCTION

The genesis of an individual axodendritic synaptic connection is a concerted process that involves structural and functional rearrangements on both sides of the nascent synaptic junction. The process begins with the formation of physical contact between potential synaptic partners. Such contacts may be initiated by axonal growth cones or by dendritic growth cones and filopodia. The axonal and dendritic compartments in the vicinity of such contact sites thereafter differentiate into presynaptic boutons and postsynaptic reception apparatuses, respectively.

The differentiation of the presynaptic compartment at the new contact site includes the clustering of synaptic vesicles (SVs) and the formation of active zones. The latter are specialized regions of the presynaptic plasma membrane, where SVs dock, fuse, and recycle. The active zone is characterized ultrastructurally as an electron dense meshwork of cytoskeletal filaments (referred to as the CAZ), which is in intimate association with the plasma membrane and into which clusters of SVs are embedded (Burns and Augustine, 1995; Garner *et al.*, 2000a; Dresbach *et al.*, 2001; Harlow *et al.*, 2001). The differentiation of the postsynaptic compartment into a functional reception apparatus involves the formation of the post synaptic density (PSD). This electron dense structure is characterized by the presence of a highly specialized cytoskeletal matrix juxtaposed to the presynaptic CAZ that serves to cluster and localize neurotransmitter receptors as well as other molecules to the postsynaptic membrane (Garner *et al.*, 2000b; Kennedy, 2000).

Over the last several years, much has been learned about the molecular composition of the CAZ and the PSD associated with glutamatergic synapses (Sheng and Pak, 1999; Kim and Huganir, 1999; Garner *et al.*, 2000a,b; Kennedy, 2000). Furthermore, studies utilizing the yeast two hybrid system and mass spectroscopic analysis (Walikonis *et al.*, 2000; Husi *et al.*, 2000) have provided important information on how higher order complexes within the CAZ and PSD can be formed from individual synaptic molecules (Sheng and Lee, 2000). Nonetheless, little is known concerning the processes that underlay the assembly of synaptic junctions during development. For example, does assembly in-

1044-7431/01 $35.00

volve sequential, *in situ* recruitment of individual components or is it realized by the insertion of preformed multimolecular complexes into pre/postsynaptic membranes? While initial studies indicate that preformed vesicular complexes play a pivotal role in the rapid formation of presynaptic neurotransmitter release sites (Ahmari *et al.,* 2000; Zhai *et al.,* 2001), it is unknown if the postsynaptic reception apparatus is assembled in a similar fashion.

One important component of the PSD is the postsynaptic scaffold molecule SAP90/PSD-95 (Cho *et al.*, 1992; Kistner *et al.,* 1993, reviewed in Garner *et al.,* 2000b; Kennedy, 2000). This molecule is part of a multi-molecular complex containing more that 77 different proteins which include the *N*-methyl-d-aspartate (NMDA) type glutamate receptor, as well as scaffolding/adaptor proteins, kinases, phosphatases, signaling molecules and cell adhesion molecules (see Garner *et al.,* 2000b; Sheng and Lee, 2000, and references therein). Given its multidomain structure [three PDZ domains, a src homology 3 (SH3) domain and a guanylate kinase like domain], it has been suggested that SAP90/PSD-95 is itself a scaffold protein that serves to cluster postsynaptic NMDA receptors and promote the assembly of macro-molecular signaling complexes. Whether SAP90/PSD-95 performs these functions is currently unclear given that NMDA receptors are still clustered and synaptic morphology is unaltered in SAP90/PSD-95 −/− knockout mice (Migaud *et al.,* 1998; see also Passafaro *et al.,* 1999), although it should be noted that the functional properties of glutamatergic synapses in these knockout mice are significantly altered.

Several findings suggest that SAP90/PSD-95 may nonetheless play important roles in synapse formation. SAP90/PSD-95 assumes a synaptic localization early during network formation (Rao *et al.,* 1998). *Discs large*, the Drosophila homologue of this molecule, was shown to have an essential role during the development of the larval neuromuscular junction (Lahey *et al.,* 1994). SAP90/PSD-95 has been found to bind to the carboxy-terminus of Neuroligin (Irie *et al.,* 1997), a molecule recently shown to display a capacity for triggering the formation of functional presynaptic specializations *in vitro* when expressed in surrogate postsynaptic targets (Scheiffele *et al.,* 2000; see also Cantallops *et al.,* 2000). This would place SAP90/PSD-95 at a potentially strategic location in a molecular cascade proposed to be initiated by the binding of Neuroligins to their presynaptic counterparts, β Neurexins (Irie *et al.,* 1997; Missler and Sudhof, 1998). A recent report (El-Husseini *et al.,* 2000b) revealed that the over expression of SAP90/PSD-95 in cultured hippocampal neurons enhances the maturation of glutamatergic synapses, increases the number of synapses formed on neurons over expressing SAP90/PSD-95, elevates the number of α-amino-3-hydroxy-5-methyl-4-isoxazole proprionate (AMPA)-type glutamate receptors in such synapses and increases the number of SVs per synapse. Finally, it has been recently suggested that the targeting of AMPA type glutamate receptors to synaptic sites is mediated by Stargazin via its associations with both SAP90/PSD-95 and AMPA receptors (Chen *et al.,* 2000). It thus seems that SAP90/PSD-95 could play important (although not necessarily exclusive) roles in orchestrating the assembly of glutamatergic synapses.

We have previously performed a retrospective immunohistochemical analysis of new synaptic junctions based on recurrent labeling with the fluorescent endocytotic marker FM 4–64 (Vardinon-Friedman *et al.,* 2000). This analysis revealed that by the time new presynaptic boutons acquire a capacity for evoked endocytosis and exocytosis, about half of them are associated with clusters of SAP90/PSD-95, suggesting that SAP90/PSD-95 is recruited to nascent synaptic junctions early during their assembly process. However, as this study was based on a retrospective immunohistochemistry analysis of fixed tissue, it did not address key questions related to the dynamics and mode of recruitment of SAP90/PSD-95 to new synaptic junctions: When is SAP90/PSD-95 recruited to new axodendritic contact sites? What are the kinetics of SAP90/PSD-95 accumulation at such sites? Is SAP90/PSD-95 recruited from cytosolic pools or from discrete transport vesicles as suggested for other components of the pre (Ahmari *et al.,* 2000; Zhai *et al.,* 2000) and post (Setou *et al.,* 2000) synapse? Clearly, an understanding of the dynamics of SAP90/PSD-95 recruitment into newly forming synapses is likely to provide fundamental clues to its role in the assembly of PSDs.

Here we describe experiments designed to address these questions. We report that new SAP90/PSD-95 clusters appear at new axodendritic contact sites within 20–60 min of contact formation. This recruitment process is rapid and seems to be completed within one hour on average. FM 4–64 labeling confirms that most new SAP90/PSD-95 clusters are juxtaposed to functional presynaptic boutons, supporting our previous findings that synaptic assembly may occur over a time scale of 1–2 h. No evidence was found for the existence of small discrete SAP90/PSD-95 transport particles. Instead, we found evidence that SAP90/PSD-95 is recruited to nascent synaptic junctions from a diffuse dendritic cytoplasmic pool of SAP90/PSD-95 that is partly cytosolic and partly associated with a light mem-

brane fraction. These studies indicate that the recruitment process of SAP90/PSD-95 to new postsynaptic sites is fundamentally different from the processes underlying the recruitment of active zone components to new presynaptic sites.

RESULTS

SAP90/PSD-95:GFP Clusters at Glutamatergic Synapses

In order to follow the dynamics of SAP90/PSD-95 accumulation at new synaptic junctions, we expressed enhanced green fluorescent protein (EGFP) tagged SAP90/PSD-95 (SAP90/PSD-95:GFP, Arnold and Clapham, 1999) in individual cultured hippocampal neurons isolated from postnatal rats, and used automated multisite time-lapse confocal microcopy to record the clustering dynamics of this fluorescent variant of SAP90/PSD-95.

In previous studies EGFP-tagged variants of SAP90/PSD-95 have been used to examine the molecular mechanisms of dendritic and postsynaptic targeting of this molecule (Arnold and Clapham, 1999; Craven *et al.*, 1999; El-Husseini *et al.*, 2000a,b) and to study long-term synaptic remodeling of glutamatergic synapses (Okabe *et al.*, 1999). In all of these studies, recombinant SAP90/PSD-95 was targeted correctly to postsynaptic sites of glutamatergic synapses. However, expression levels varied greatly from one study to another, ranging from 37% over baseline levels (Okabe *et al.*, 1999) to 5–10 times greater than endogenous expression levels (Craven *et al.*, 1999; El-Husseini *et al.*, 2000b). In the context of the current study, high expression levels would be undesirable, as they significantly alter functional and structural characteristics of glutamatergic synapses made on those neurons overexpressing SAP90/PSD-95 (El-Husseini *et al.*, 2000b). It was thus important to determine the degree to which the overall levels of SAP90/PSD-95 were altered by the expression of SAP90/PSD-95:GFP in our system and to determine if these expression levels were associated with significant alterations of synaptic characteristics.

To that end, we collected images of neurons expressing SAP90/PSD-95:GFP. These neurons were then fixed, immunostained, and subjected to quantitative analysis. An individual neuron expressing SAP90/PSD-95:GFP is shown in Figs. 1A–1E. As previously reported, SAP90/PSD-95:GFP displays a punctate distribution, accumulating at what seem to be shaft and spine postsynaptic sites. Immunostaining against SAP90/PSD-95 was used to compare the average levels of SAP90/PSD-95 in such puncta to those of neurons in the same dishes that did not express SAP90/PSD-95:GFP. Overall, the anti-SAP90/PSD-95 staining levels in puncta of neurons expressing SAP90/PSD-95:GFP were only 27% higher on average than those of naive neurons in the same culture dish, suggesting that the overall levels of SAP90/PSD-95 in neurons expressing SAP90/PSD-95:GFP were only modestly affected. Interestingly, a comparison of SAP90/PSD-95:GFP intensity and anti-SAP90/PSD-95 staining in individual clusters revealed a linear relationship between these two measures (with an intercept at the origin), suggesting that the endogenous and exogenous molecules were well mixed (Figs. 1F and 1G). Note that the slope varies slightly in different cells in the same dish, suggesting that the relative expression levels of endogenous and exogenous SAP90/PSD-95 varied slightly from one neuron to another.

Staining with antibodies against the AMPA receptor subunit 1 (GluR1) revealed that most (84% on average) of SAP90/PSD-95:GFP clusters colocalize with clusters of GluR1 (Fig. 2A). Quantitative analysis of immunostained GluR1 clusters revealed a small but statistically significant elevation (16%) of the mean staining intensity of GluR1 clusters formed on neurons expressing SAP90/PSD-95:GFP as compared to GluR1 cluster staining intensity in naive neurons in the same dish ($n = 253$ and 325, respectively, Mann–Whitney rank sum test). Staining against MAP-2, a specific dendritic marker (Caceres *et al.*, 1984), suggested that SAP90/PSD-95:GFP clusters were limited to dendrites (Fig. 2B), as all processes decorated with SAP90/PSD-95:GFP clusters were also MAP-2 positive.

When FM 4–64 and field stimulation were used to label synaptic vesicles in functional presynaptic boutons (Vardinon-Friedman *et al.*, 2000; see also Cochilla *et al.*, 1999) as shown in Fig. 2C, most SAP90/PSD-95:GFP clusters were observed to be associated with functional presynaptic boutons (83%, $n = 868$, 11 sites, 5 separate experiments). No statistically significant differences were observed between dye uptake in such boutons to those measured in boutons not associated with SAP90/PSD-95:GFP clusters (392 and 1133 boutons, respectively, 9 sites, 3 separate experiments, Mann–Whitney rank sum test).

These findings show that SAP90/PSD-95:GFP is targeted to bona fide synaptic junctions, and that the expression levels of the exogenous SAP90/PSD-95 variant used here were not unacceptably high. In agreement with a previous report (El-Husseini *et al.*, 2000b), we did observe an increase in the number of postsynaptic

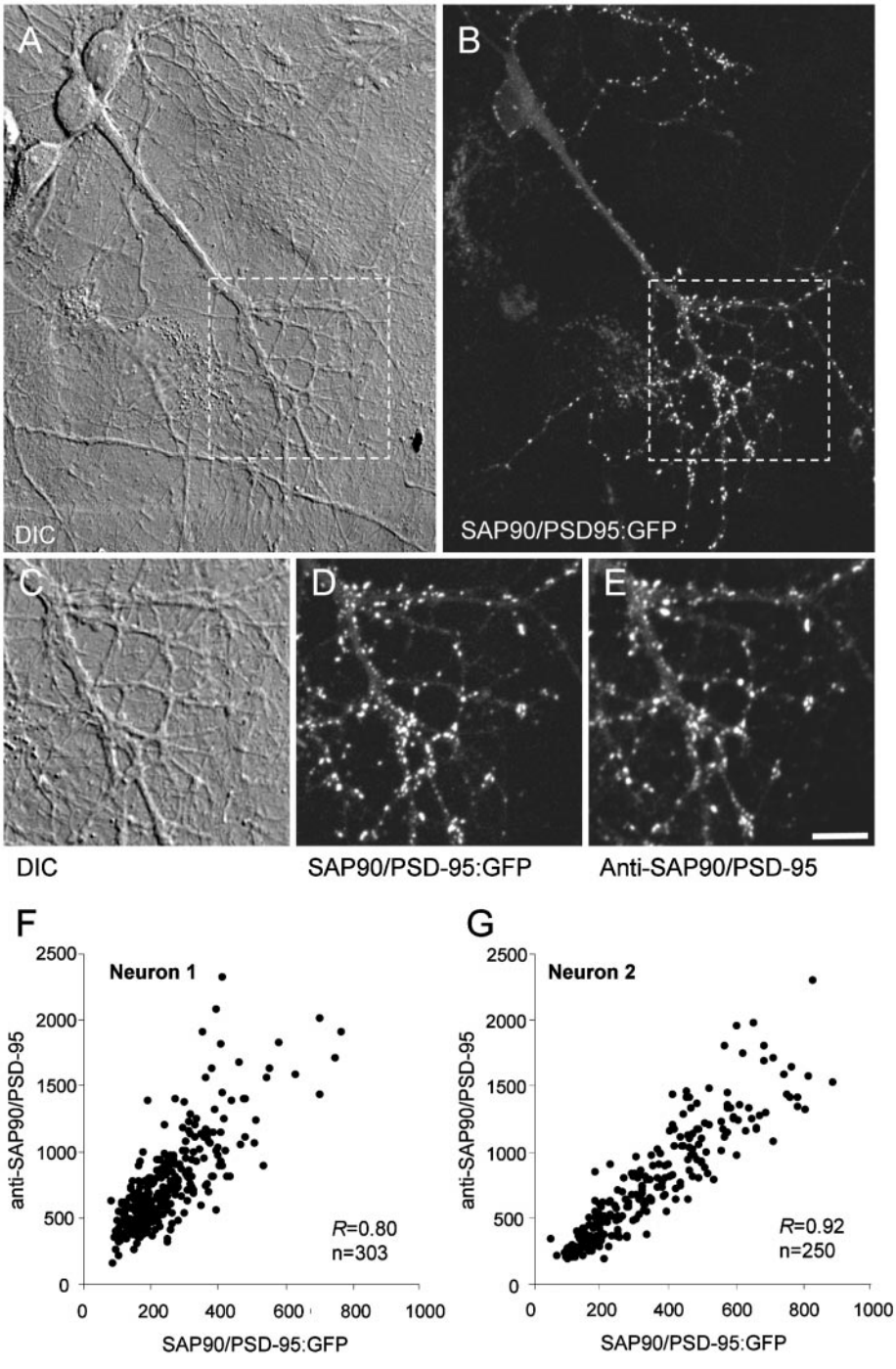

FIG. 1. SAP90/PSD-95:GFP expressed in cultured hippocampal neurons is targeted to synaptic sites. (A) A differential interference contrast (DIC) image of postnatal hippocampal neurons grown in culture for 12 days. (B) A single neuron in the field, expressing SAP90/PSD-95:GFP. Transfection was carried out on day 7 *in vitro*. (C) Higher magnification of region enclosed in rectangle in A. (D) Higher magnification of region enclosed in rectangle in B. Note the punctate staining pattern of the fluorescent molecule. (E) Same region as in D after fixation and staining with antibodies against SAP90/PSD-95. Images in A–D obtained prior to fixation. Bar, 10 μm. (F, G) Comparison of SAP90/PSD-95:GFP fluorescence and anti SAP90/PSD-95 staining in individual puncta reveals that these two measures are highly correlated, suggesting that endogenous and exogenous forms of SAP90/PSD-95 are well mixed at most PSDs. The tendency of imaginary trendlines to cross the ordinate near 0 argues against the existence of a significant population of PSDs devoid of SAP90/PSD-95:GFP. Puncta intensities were determined by averaging the intensity values of the 3 $\times$ 3 pixels at the center of each cluster. *R*, correlation coefficient. *n*, number of data points in each graph.

AMPA type glutamate receptors per cluster. This effect, however, was much smaller than that previously reported. Furthermore, we did not detect significant presynaptic effects. We thus conclude that the expression of SAP90/PSD-95:GFP is a valid method for studying the recruitment of SAP90/PSD-95 to nascent synaptic junctions.

SAP90/PSD-95 Does Not Seem to Be Transported within Discernable Vesicles

Recent studies have provided evidence suggesting that the assembly of presynaptic actives zone may be realized by the insertion of preassembled, multimolecular complexes into the synaptic membrane (Ahmari *et al.*, 2000; Zhai *et al.*, 2001; see also Roos and Kelly, 2000). These complexes are carried on discrete vesicles that are readily discernable in fixed and immunofluorescently stained hippocampal neurons. Similarly, subunits of postsynaptic NMDA glutamate receptors were shown to be carried on transport vesicles (Setou *et al.*, 2000), which could explain the punctate distribution pattern these molecules display in dendrites long before synapses form (Rao and Craig, 1997; Rao *et al.*, 1998).

Is SAP90/PSD-95 transported to nascent synapses in a similar fashion? When SAP90/PSD-95:GFP is expressed in nonneuronal cell lines, it is observed to concentrate at perinuclear compartments and seems to exhibit trafficking through pleomorphic vesiculotubular structures (El-Husseini *et al.*, 2000a). Furthermore, correct targeting of SAP90/PSD-95 to synaptic sites requires dual palmitoylation at the NH_2 terminus (Craven *et al.*, 2000; El-Husseini *et al.*, 2000a). This has lead to the suggestion that SAP90/PSD-95 is an itinerant vesicular protein and that its targeting to an intracellular membranous compartment is required for its clustering at synaptic sites (El-Husseini *et al.*, 2000a).

To determine if mobile, presumably vesicular, clusters of SAP90/PSD-95 are present in neuronal dendrites, we performed time-lapse recordings of neurons grown for 8–12 days *in vitro* and expressing SAP90/PSD-95:GFP. These experiments revealed that most SAP90/PSD-95:GFP clusters were rather static over long durations (many minutes to hours). Furthermore, time lapse recordings performed at short intervals (4 to 60 s) failed to uncover a population of highly mobile clusters of SAP90/PSD-95:GFP (data not shown). However, time-lapse recordings performed at 10 to 20 min intervals revealed that some SAP90/PSD-95:GFP clusters displayed significant longitudinal movements, up to 5 μm over 10 min (Figs. 3, 4, see also Fig. 6A). The movement rates of these clusters were much lower than those typically associated with vesicles propelled along microtubules by molecular motors (0.1–10 μm/s; Goldstein and Yang, 2000). These movements were nevertheless quite significant. Furthermore, the size of the mobile clusters was not noticeably different from the size of the relatively static clusters, which lead us to suspect that these movements represent changes in the position of entire synaptic structures.

To further explore the nature of these movements, we labeled functional presynaptic boutons in the preparations using FM 4–64 and field stimulation as in Fig. 2C. Then, time lapse recordings were performed in order to follow concomitantly clusters of SAP90/PSD-95:GFP and presynaptic boutons. These experiments clearly revealed that in almost all cases, the mobile SAP90/PSD-95:GFP clusters were juxtaposed against clusters of FM 4–64-labeled vesicles, and that the pre and postsynaptic structures moved in unison, as shown in Fig. 4.

Although these observations substantiated our suspicions that the slow longitudinal movements of SAP90/PSD-95:GFP reflected changes in the position of entire synaptic structures, it remained possible that a small population of (relatively) mobile clusters were nonsynaptic, possibly constituting some form of transport particle. We thus quantified the average mobility of each SAP90/PSD-95:GFP cluster, grouped the clusters according to their mobility, and determined the fraction of clusters within each group that were matched with functional presynaptic boutons as determined by their capacity to uptake and release FM 4–64 in response to electrical stimulation. As shown in Fig. 4B, no significant differences were found among the various groups. Thus, the slow longitudinal movement of SAP90/PSD-95:GFP clusters does not seem to reflect a transport process, and probably reflects synaptic movement resulting from mechanical forces induced by elongating axons and dendrites tugging in different directions, by dendritic and axonal cytoskeletal dynamics, or movements of underlying glial cells.

Interestingly, similar experiments performed with a GFP-tagged preproatrial natriuretic protein (ANP:GFP) gave strikingly different results. This molecule has been previously shown to be packaged in secretory granules that are subsequently transported to neurite endings when expressed in PC12 cells (Burke *et al.*, 1997; Han *et al.*, 1999). Although the expression pattern of ANP:GFP in hippocampal neurons was also punctate, these puncta were extremely mobile, moving at rates reaching ~15 μm/min (Fig. 4C) and did not colocalize with FM 4–64-labeled presynaptic boutons (data not shown). Retrospective staining with MAP2, as in Fig. 2B, confirmed that these puncta, most likely secretory vesicles of some form,

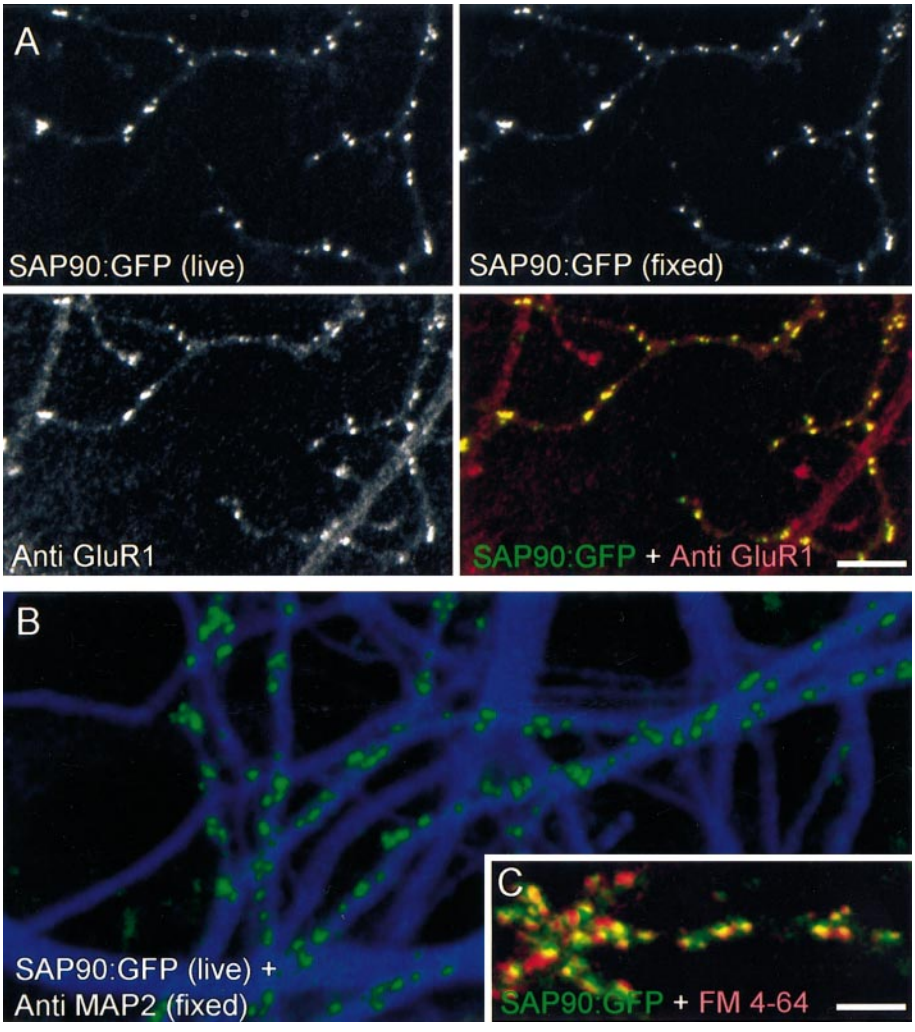

FIG. 2. SAP90/PSD-95:GFP clusters are postsynaptic and are associated with functional presynaptic boutons. (A) Retrospective staining of neurons expressing SAP90/PSD-95:GFP with antibodies against the AMPA-type glutamate receptor subunit GluR1. Note the excellent correspondence between clusters of SAP90/PSD-95:GFP and GluR1, suggesting that most SAP90/PSD-95:GFP clusters are localized to glutamatergic synapses. (B) Retrospective staining of neurons expressing SAP90/PSD-95:GFP (green) with antibodies against the specific dendritic market MAP2 (blue) confirms the dendritic localization of SAP90/PSD-95:GFP puncta. (C) Labeling of functional presynaptic boutons with FM 4–64 (red) reveals that most SAP90/PSD-95:GFP clusters (green) are associated with functional presynaptic boutons. Bars, 10 μm (A), 5 μm (B, C).

were being transported along dendritic processes (data not shown). Although ANP is an exogenous molecule, its use in these experiments was instrumental for providing some idea as to the characteristics of fast dendritic transport processes in cultured hippocampal neurons, and served to demonstrate that if SAP90/PSD-95:GFP had exhibited similar characteristics, this would have been detected in our system.

To summarize, we found no evidence in favor of the possibility that SAP90/PSD-95 is transported along dendrites within readily discernable transport vesicles as shown for other PSD components such as NMDA receptor subunit 2 (Setou *et al.*, 2000) or presynaptic CAZ components such as Bassoon and Piccolo (Zhai *et al.*, 2001), suggesting that SAP90/PSD-95 is recruited to nascent synaptic junctions in an alternative fashion.

Dendritic SAP90/PSD-95 Is Found in Both Light Membranal and Cytosolic Fractions

In addition to the punctate synaptic distribution observed on somata and dendritic profiles of neurons

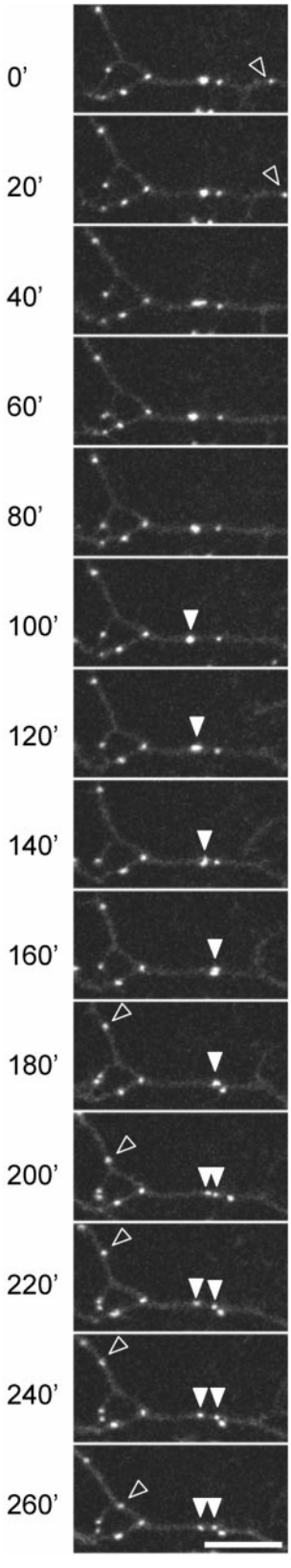

transfected with SAP90/PSD-95:GFP, a weak but significant diffuse, nearly uniform, fluorescence was also observed within the same dendrites. As we found no evidence for discernable SAP90/PSD-95:GFP transport particles/vesicles, it seemed plausible that this diffuse fluorescence arose from potential pools from which SAP90/PSD-95 is recruited to new synaptic junctions. To determine if the source of this fluorescence was SAP90/PSD-95:GFP associated with the plasma membrane, we examined single confocal sections as well as intensity profiles of dendritic cross sections. These data suggested that most of the diffuse fluorescence resided in the cytoplasm, not the plasma membrane. This conclusion was also supported by the finding that fluorescence intensity measured at the center of dendrites scaled linearly with dendritic diameter (as exemplified in Fig. 5), which is consistent with the fluorescence originating in the cytoplasm but inconsistent with the fluorescence originating primarily in the plasma membrane. In agreement with previous studies (Rao *et al.*, 1998), we observed similar staining in naive neurons immunostained against SAP90/PSD-95, indicating that the diffuse cytoplasmic staining is not an artifact of SAP90/PSD-95:GFP expression (data not shown).

The cytoplasmic location of diffuse SAP90/PSD-95 fluorescence does not necessarily indicate that it originates from a soluble cytosolic pool. It could also originate from SAP90/PSD-95 associated with intracellular vesicular membranes too dim, complex or numerous to be resolved by light microscopy. We therefore examined to what extent SAP90/PSD-95 exists in cytosolic, vesicular membrane and/or synaptic junctions during the peak period of synaptogenesis in the developing rat brain. The partitioning of SAP90/PSD95 between cytosolic and total membranes was assessed by Western blotting the 100,000*g* supernatant and membrane pellet fractions from embryonic day 19 (E19) and postnatal days 2, 4, 8, 10, and 20 rat brain homogenates. In these experiments, the membrane pellet fractions were resuspended in an equal volume of buffer as the volume of supernatant allowing a direct comparison of the relative

FIG. 3. Longitudinal movements of SAP90/PSD-95:GFP clusters. Time lapse of SAP90/PSD-95:GFP clusters reveal that most clusters are stable. Some clusters, however, display slow longitudinal movements (arrowheads) that are often bidirectional (open arrowhead, t = 200 and onward). In some cases clusters move into close proximity of other clusters, and it becomes difficult to resolve with certainty their identity and direction of travel after such events (closed arrowheads). In addition, clusters sometimes appear to split into several smaller clusters (closed arrowheads, t = 200 and onward). Bar, 10 μm.

amounts of SAP90/PSD-95 in these two fractions. At all days examined only 25% of the SAP90/PSD-95 was found in the supernatant fraction with the remaining 75% cofractionating with the membrane fraction (Fig. 6A). This ratio did not change during the first three weeks of postnatal life, suggesting that a quarter of SAP90/PSD-95 exists in a soluble form within the neuronal cytoplasm. This contrasts somewhat to the integral membrane protein synaptophysin that is found in the pellet fractions (Zhai *et al.,* 2001).

The association of SAP90/PSD-95 with light microsomal membranes versus synaptosomal was evaluated with a flotation assay (Zhai *et al.,* 2001). This was accomplished by resuspending the 100,000*g* membrane pellet fraction from different ages in 2 M sucrose and placing these samples at the bottom of a discontinuous 0.3 to 2 M sucrose gradient. After centrifugation at 50,000*g* for 3 h, 0.5-ml fractions taken from the top of the gradient were separated by SDS–PAGE and Western blotted. In this assay, SAP90/PSD-95 present in P2 and P4 rat brain homogenates was found in fractions 3–7 in a pattern similar to synaptophysin (Fig. 6B). Resuspending the pellet fraction in 2 M sucrose containing 1% Triton X-100, before centrifugation, caused both SAP90/PSD-95 (Fig. 6B) and synaptophysin (data not shown) to remain at the bottom of the gradient, fractions 6–7. This condition which serves to disrupt membranes indicates that the presence of SAP90/PSD-95 in the upper fractions is due to its association with light "microsomal" membranes. This conclusion is supported by similar experiments on SAP90/PSD-95 in the supernatant fractions. Here, SAP90/PSD-95, in the absence of Triton X-100, remains at the bottom of the gradient. The analysis of membrane fractions from older animals (P20) revealed a general shift of SAP90/PSD-95 to the bottom of the gradient (data not shown). A similar age-dependent shift from light to heavy membrane fractions has also been seen with the presynaptic active zone protein, Piccolo (Zhai *et al.,* 2001). This appears to reflect the recruitment of these proteins into synaptic junctions which, in synaptosomal form, are known to have a lower buoyant density. Taken together, these data indicate that prior to its recruitment into synapses, SAP90/PSD-95 is both cytosolic and associated with intracellular membranes.

The Dynamics of de Novo SAP90/PSD-95 Cluster Formation

To determine if the formation of new SAP90/PSD-95 clusters is consistent with a gradual recruitment from the diffuse cytoplasmic pool described above, we performed time-lapse recordings of neurons expressing SAP90/PSD-95:GFP, and followed the formation of new SAP90/PSD-95:GFP clusters. We typically performed these experiments at relatively low sampling rates (one sample per 10–20 min) as we found that these sampling rates provide a good compromise between adequate sampling frequency and long term survivability of the preparations. These experiments revealed that new SAP90/PSD-95 clusters originated from (1) the splitting of existing SAP90/PSD-95 clusters into two or more smaller clusters; (2) the *de novo* formation of new clusters along preexisting dendritic segments or along new dendritic structures formed by dendritic growth cones.

The formation of new SAP90/PSD-95 clusters by splitting of preexisting clusters (as may be seen in Fig. 3) has been described previously (Marrs, Green, and Dailey, Abstracts of the Society for Neuroscience, 2000) and was not examined further in the current study. Our efforts here were focused on the *de novo* formation of SAP90/PSD-95 clusters, as illustrated by examples shown in Figs. 7 and 8. In the first example (Fig. 7, lower panels), a new, discrete cluster of SAP90/PSD-95:GFP was observed to form along a preexisting dendritic segment. In the second example (Fig. 7, upper panels), a new cluster of SAP90/PSD-95:GFP was formed on an advancing dendritic growth cone, in a manner reminiscent of the formation of presynaptic terminals behind advancing axonal growth cones (Jontes *et al.,* 2000). In the third example (Fig. 8) a new cluster of SAP90/PSD-95:GFP formed rapidly at the intersection between an elongating axon and an elongating dendrite.

In all events in which the *de novo* formation SAP90/PSD-95 clusters was recorded, the new clusters seemed to form by a gradual accumulation of fluorescent material from some diffuse source, never from the trapping or coalescing of discernable, discrete fluorescent clusters. A quantitative analysis of this process was performed by measuring changes in the total fluorescence within a square box (1.5×1.5 μm) centered on the new clusters. Although single cluster recordings were typically quite noisy (as shown in Figs. 7B and 7C), the time course of SAP90/PSD-95 recruitment emerged when normalized data from 56 new clusters was pooled together (see Experimental Methods). As shown in Fig. 7D, the recruitment process is quite abrupt, nearly plateaus after 1 h, and can be fit with a single exponential with a time constant of 23 min. In contrast, the mean intensity of preexisting clusters did not change much over time, except for a slight time-dependent decrease, probably caused by photobleaching.

These experiments suggest that new SAP90/PSD-95 clusters are formed by the rapid recruitment of SAP90/PSD-95 from some diffuse cytoplasmic pool and that the increase in cluster size displays a time course that can be described quite well by a single exponential.

SAP90/PSD-95 Accumulates Rapidly at New Synaptic Junctions

Many of the new SAP90/PSD-95:GFP clusters whose appearance was recorded appeared along new dendritic segments formed by advancing dendritic growth cones. In some cases, the new cluster first appeared at the tip of a filopodium extending from the dendritic growth cone (Fig. 7A, upper panels). The new SAP90/PSD-95 clusters first appeared 20–60 min after the dendritic growth cones or filopodia first reached the location at which the new clusters subsequently appeared (mean = 36 min, $n = 14$). We assume that these clusters had formed at sites where the advancing growth cones had intersected axons, and indeed, in some cases (4), faintly fluorescent axons were discernable at these locations (as in Fig. 8). In other cases, however, axons were not resolved at these sites by fluorescence microscopy (i.e., Fig. 7A, upper panels). Although this is expected given that only a small fraction of neurons expressed the fluorescent molecule, the lack of discernable presynaptic partners may also be interpreted to suggest that some of the new SAP90/PSD-95 clusters had formed at non-synaptic sites.

To determine if the formation of new SAP90/PSD-95:GFP clusters reflected the recruitment of this molecule to bona fide synaptic sites, we complemented time-lapse recordings of neurons expressing SAP90/PSD-95:GFP with FM 4–64 labeling of presynaptic boutons as described above (see Figs. 2 and 4). These experiments revealed that most new SAP90/PSD-95:GFP clusters were associated with functional presynaptic boutons as determined by their capacity to uptake and release FM 4–64 in response to evoked stimulation. One rather striking example is shown in Fig. 9. In this example, a small dendritic branch was observed to extend laterally from a larger dendrite. As this branch elongated, four new SAP90/PSD-95:GFP clusters were formed sequentially at increasing distances from the main dendrite. Labeling of functional boutons with FM 4–64 at the end of the experiment revealed that all four new clusters were associated with functional presynaptic boutons.

Altogether, the formation of 23 new SAP90/PSD-95:GFP clusters was recorded in these experiments. 58% of new SAP90/PSD-95:GFP clusters were found to be associated with functional boutons within 1 h of their appearance ($n = 12$), while 91% were associated with functional boutons within 4 h of their appearance ($n = 11$). We thus conclude that new SAP90/PSD-95 clusters can form within 20–60 min of axodendritic contact and that the large majority of new SAP90/PSD-95:GFP clusters observed to form in our experiments had indeed formed at nascent synaptic junctions.

DISCUSSION

We have used GFP-tagged SAP90/PSD-95, time lapse confocal microscopy, and cultured hippocampal neurons to study the manner by which SAP90/PSD-95 is recruited to new synaptic junctions. We established that SAP90/PSD-95:GFP clusters at bona fide postsynaptic sites and determined that the expression of this exogenous molecule in our system does not seem to have a large impact on synaptic characteristics previously shown to be sensitive to SAP90/PSD-95 overexpression. Our experiments did not uncover evidence for the transport of SAP90/PSD-95 in discrete packets, but we have found evidence for a diffuse cytoplasmic pool of SAP90/PSD-95 in dendrites, partly cytosolic and partly associated with a light membrane fraction. Time lapse recordings suggest that new SAP90/PSD-95 clusters form by the recruitment of SAP90/PSD-95 from this diffuse dendritic pool. Quantitative analysis reveals that the recruitment is rapid, with an average time constant of ~23 min. New SAP90/PSD-95 clusters formed at new axodendritic contact sites within 20–60 min of contact establishment, and in most cases were associated with functional presynaptic boutons. The rapid recruitment of SAP90/PSD-95 to new synaptic junctions supports previous suggestions that SAP90/PSD-95 has a role in orchestrating the assembly of the postsynaptic density. Our findings indicate, however, that this assembly process may be fundamentally different from the assembly process of the presynaptic active zone cytoskeleton.

The Time Course of New SAP90/PSD-95 Cluster Formation

Our analysis reveals that SAP90/PSD-95 clusters at new synaptic sites, defined by their ability to recycle synaptic vesicles in an activity-dependent manner, with a mean time constant of ~23 min. This data was collected at near optimal conditions, i.e., at 37°C, without perfusion-related perturbations, in conditioned growth media, and in an atmospheric environment similar to that of tissue culture incubators, suggesting that these

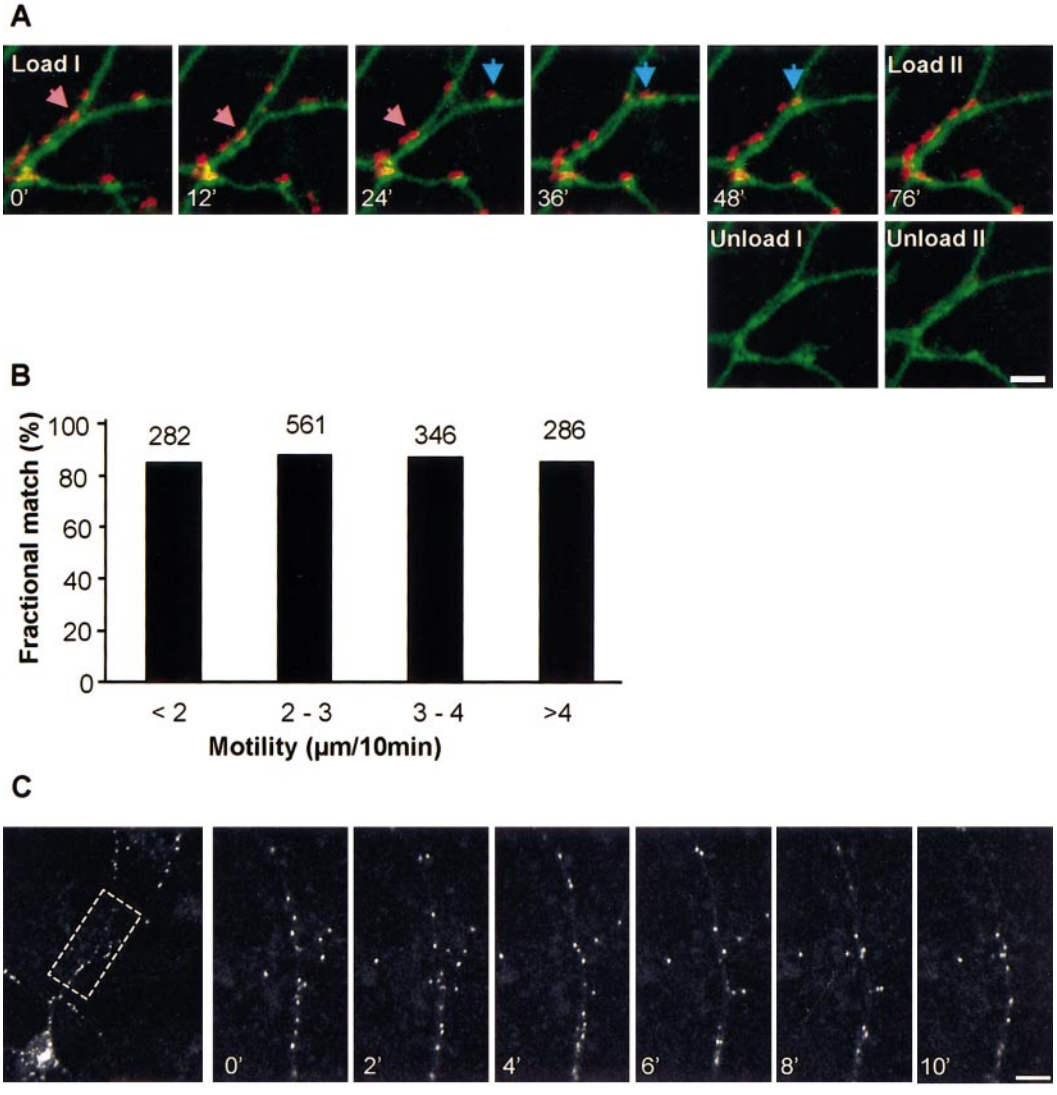

FIG. 4. Most slow longitudinal movements of SAP90/PSD-95:GFP clusters represent the migration of entire synapses. (A) Concomitant imaging of SAP90/PSD-95:GFP clusters (green) and functional presynaptic boutons labeled with FM 4–64 (red) reveals that the slow migration of SAP90/PSD-95:GFP clusters usually occurred in unison with the migration of the presynaptic bouton associated with this cluster (pink and cyan arrows, two separate synapses). The functional status of these presynaptic boutons was confirmed by releasing the dye trapped within presynaptic vesicles by a train of action potentials (Unload I, 120 s at 10 Hz), reloading them with FM 4–64 (Load II), and unloading them again (Unload II). For purposes of clarity the FM 4–64 images shown here were offset by 5 pixels to the left and 5 pixels to the top relative to the SAP90/PSD-95:GFP images. Bar, 5 μm. (B) Quantitative analysis revealed no significant correlation between the average longitudinal mobility displayed by a SAP90/PSD-95:GFP cluster and the probability that the cluster is associated with a functional presynaptic bouton, arguing against the existence of a significant population of mobile, nonsynaptic, SAP90/PSD-95:GFP clusters. All data was obtained from neurons grown in culture for 8–12 days. (C) Expression of ANP:GFP in hippocampal neurons. Left panel, low magnification image of a cultured hippocampal neuron expressing ANP:GFP. Note the punctate distribution of the fluorescent neuropeptide along the dendritic segments shown here (the dendritic identity of these segments was confirmed by retrospective staining with MAP2, not shown here). Time lapse sequence of the region enclosed in rectangle is shown in the right-hand panels. Note the high degree of mobility displayed by ANP:GFP clusters (the inter-frame time interval here is only 2 min). In fact, the mobility displayed by these puncta (presumably vesicles of some sort) precluded the display of maximal intensity projections of image stacks, as puncta changed their position during the time required to collect an image stack, thus only single sections are displayed here. Bar, 5 μm.

experiments provide a reasonable approximation of physiological rates of SAP90/PSD-95 clustering at new synaptic sites. Yet we cannot completely rule out the possibility that the rapid accumulation rates are somehow related to the use of SAP90/PSD-95:GFP or cell cultures. Interestingly, the formation of new SAP90/

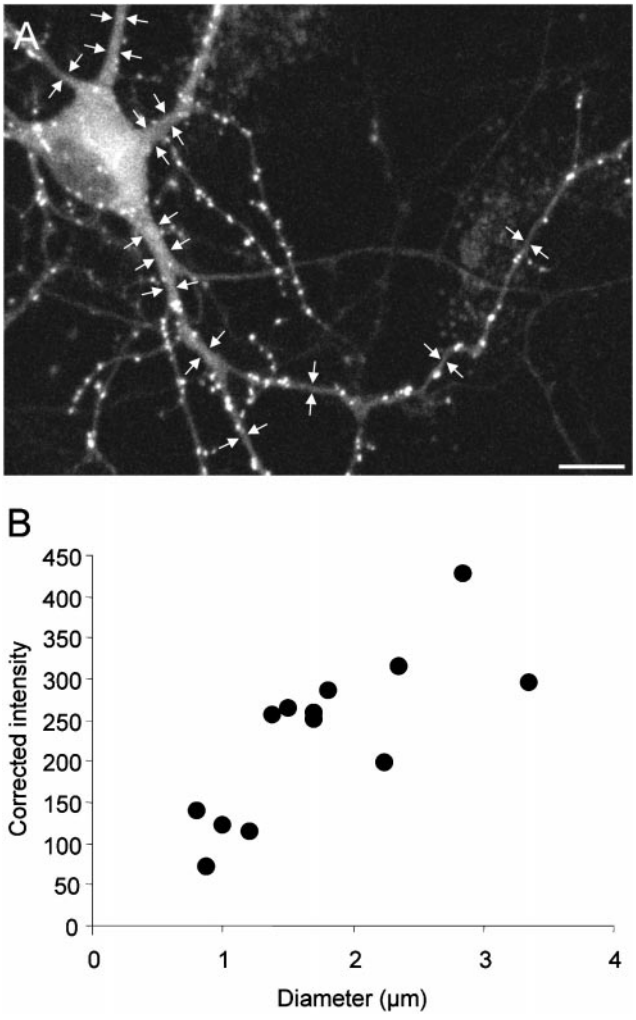

FIG. 5. Diffuse dendritic fluorescence of SAP90/PSD-95:GFP originates in cytoplasm. (A) A summed intensity projection of 4 sections spaced 1.2 μm apart of a hippocampal neuron expressing SAP90/PSD-95:GFP. Note that the diffuse fluorescence is not brighter along the dendrite's sides. (B) The intensity of the diffuse dendritic fluorescence was measured at 13 points along the dendrite indicated by arrow pairs in A. In all cases the intensity was measured from a narrow region at the center of the dendrite (between the arrow pairs). Background fluorescence values were then measured outside the dendrite for each region separately, and subtracted from the measurements made for these regions. The corrected data was then compared with the diameter of the dendrite at the point of measurement. This comparison revealed a linear relationship between dendrite diameter and diffuse fluorescence intensity suggesting that this diffuse fluorescence originates in the cytoplasm, not the dendritic plasma membrane. Bar, 10 μm.

PSD-95 clusters in older and more stable hippocampal cultures seems to occur much more slowly, on a time scale of hours (Okabe *et al.*, 1999). We suspect that the different kinetics may reflect a difference in the abundance of SAP90/PSD-95 free to accumulate at new sites.

The relatively rapid recruitment of SAP90/PSD-95 to new synaptic sites is in agreement with a prior study we performed in which FM 4–64 labeling was used to detect new functional presynaptic boutons and retrospective immunohistochemistry was used to analyze the composition of these presumably new synaptic junctions (Vardinon-Friedman *et al.*, 2000). This analysis revealed that by the time such new presynaptic boutons acquire a capacity for evoked endocytosis and exocytosis, about half of them are associated with clusters of SAP90/PSD-95. We proposed that the recruitment of SAP90/PSD-95 to nascent synapses may be delayed in respect to the formation of the presynaptic bouton, but we also pointed out that these findings are consistent with the possibility that presynaptic bouton formation and SAP90/PSD-95 recruitment occur in parallel. Our current finding that about 60% of new SAP90/PSD-95 clusters are associated with functional presynaptic boutons within one hour tends to support the latter possibility. In any case, the current study (and in particular observations such as those in Fig. 8) strongly support our previous conclusions that new glutamatergic synapses may form rapidly, within 1–2 h from contact establishment (Vardinon-Friedman *et al.*, 2000; see also Ahmari *et al.*, 2000).

Source of SAP90/PSD-95 Recruited to New Synaptic Sites

We have not found any evidence for the existence of a population of discrete transport vesicles containing SAP90/PSD-95 or for the assembly of new SAP90/PSD-95:GFP puncta by the coalescence of small discrete clusters. It could be argued that such events could have been missed by the relatively slow sampling rate we typically used (one sample per 10–20 min). As noted above, however, time-lapse recordings performed at higher sampling rates (up to one sample per 4 s) failed to reveal the existence of a dynamic pool of transport particles even remotely similar to those observed in neurons expressing ANP:GFP.

We assume that the diffuse cytoplasmic SAP90/PSD-95 observed in dendrites is composed of cytosolic SAP90/PSD-95, but we cannot rule out that this diffuse distribution also reflects SAP90/PSD-95 associated with membranal organelles too dim, too numerous or too convoluted to be resolved at the light microscopy level. Indeed, our biochemical analysis points to the existence of two pools of SAP90/PSD-95, one cytosolic and a second associated with light membranes (Fig. 6). It is worth noting that AMPA-type glutamate receptors, that are integral membranal proteins, also display a diffuse,

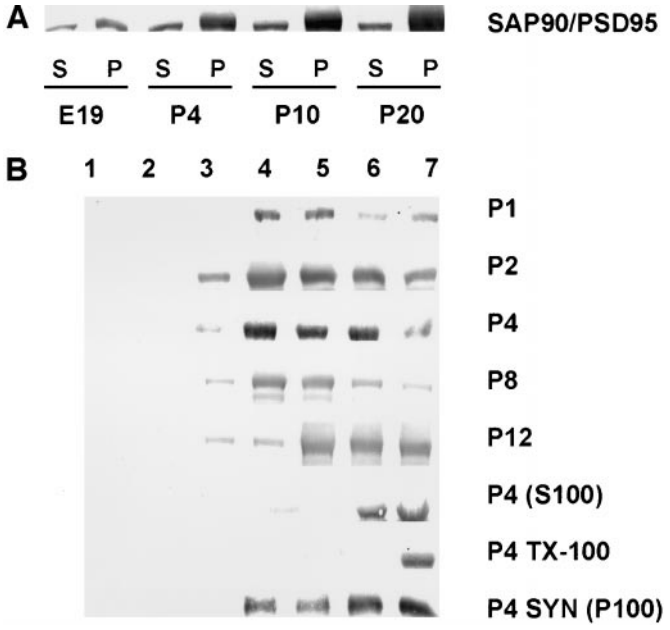

FIG. 6. Fractionation of SAP90/PSD-95 in developing rat brain homogenates. (A) Western blots of Pellet (P100) and supernatant (S100) fractions of from E19, P4, P10, and P20 rat brains homogenate stained with mouse SAP90/PSD-95 antibodies. (B) Western blots of P100 or S100 fractions from either P1, P2, P4, P8, or P12 rat brain homogenates after running on a flotation gradient and stained with antibodies against SAP90/PSD-95 or synaptophysin (SYN). Gradients were prepared by adjusting P100 or S100 fractions with 2 M sucrose and loading them at the bottom of a sucrose gradient of 0.3, 0.8, and 1.2 M. After centrifugation fractions were taken from the top (fraction 1) of the gradient to the bottom (fraction 7). In membrane disruption experiment, P100 was also treated with 1% Triton X100 (TX) for 30 min before adjusted to 2 M sucrose.

uniform dendritic distribution before and during periods of peak synaptogenesis (Craig *et al.*, 1993; O'Brien *et al.*, 1997; Mammen *et al.*, 1997; Rao *et al.*, 1998; Shi *et al.*, 1999), suggesting that a diffuse distribution does not necessarily imply a cytosolic location. Thus even though we have not found evidence for discrete transport particles containing SAP90/PSD-95, it remains possible that SAP90/PSD-95 is recruited from some diffuse, membrane associated pool. Interestingly, we found that the total fluorescence of typical new SAP90/PSD-95:GFP clusters is equivalent to the total fluorescence of about 3 cubic micrometers of dendritic cytoplasm (data not shown). Assuming that all SAP90/PSD-95:GFP, in a volume of $1 \times 1 \times 3$ μm, is within vesicles spaced 1 μm apart from another and distributed evenly within this volume, the total number of vesicles in this volume would be 16. Given the spatial resolution of our confocal microscope system, vesicles distributed in this manner would have been resolved. Yet as they were not, this suggests that at least 16 vesicles (and probably many more if somewhat less conservative values are used) would be required for the formation of a new synaptic cluster of SAP90/PSD-95. This is a fundamental difference from the assembly process of presynaptic active zones, where one active zone precursor vesicle may be sufficient for the formation of one to three new SV release sites (Zhai *et al.*, 2001).

As mentioned before, SAP90/PSD-95:GFP expressed in nonneuronal cell lines (or very immature cultured hippocampal neurons) was shown to concentrate at perinuclear compartments and dual palmitoylation was found to be crucial for both association with such membranous organelles and for proper clustering of SAP90/PSD-95 at synaptic sites (El-Husseini *et al.*, 2000a). Yet immunohistochemical analysis revealed that these perinuclear compartments corresponded very well with staining against mannose 6-phosphate receptor, a key molecule involved in sorting and shuttling lysosomic enzymes (Hille-Rehfeld, 1995). This may be interpreted to suggest that SAP90/PSD-95 observed to accumulate at these perinuclear locations was in the process of being degraded rather than being shuttled out to the periphery. Thus, further work is required to clarify the nature of membrane-associated fractions of SAP90/PSD-95 and their roles in PSD assembly.

The Roles of SAP90/PSD-95 in Synaptic Assembly

The current study suggests that SAP90/PSD-95 clusters at nascent synaptic junctions early during their formation (see also Rao *et al.*, 1998). It is interesting to note in this regard that SAP90/PSD-95 has been shown to bind via it's third PDZ domain to the carboxy-terminus of Neuroligin (Irie *et al.*, 1997), a molecule that displays a capacity to induce presynaptic specialization formation (Scheiffele *et al.*, 2000). It is therefore tempting to speculate that the rapid clustering of SAP90/PSD-95 that we observed is triggered by the binding of Neuroligin to its axonal counterparts, presumably members of the Neurexin family (Missler and Sudhof, 1998) and that SAP90/PSD-95 in turn induces the recruitment of downstream molecules. This concept is not supported by studies showing that SAP90/PSD-95 variants in which the third PDZ domain has been deleted still cluster at synaptic sites (Craven *et al.*, 1999). One intriguing interpretation may be that Neuroligin is recruited to synaptic sites by SAP90/PSD-95 and not vice versa. This could explain why presynaptic boutons made on neurons overexpressing SAP90/PSD-95 were

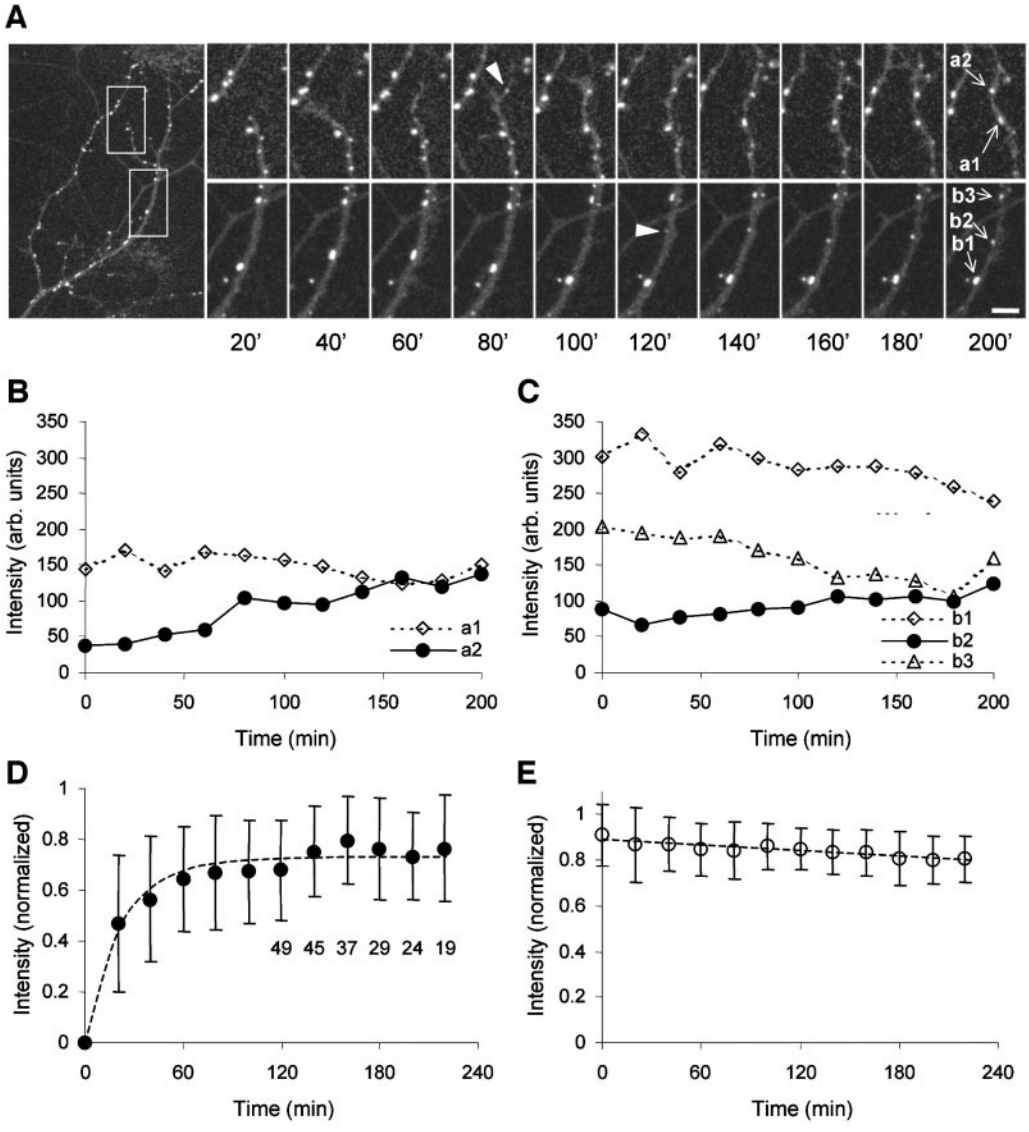

FIG. 7. Formation of new SAP90/PSD-95:GFP clusters. (A) Time lapse sequences showing the appearance of new clusters of SAP90/PSD-95:GFP. In the top time-lapse sequence (upper rectangle in low magnification image on left hand side) a new cluster of SAP90/PSD-95:GFP has formed on a filopodium extending from the leading edge of an elongating dendritic growth cone (arrowhead). In subsequent images, the growth cone advances, and the cluster becomes part of the new dendrite formed behind the growth cone. Interestingly, this sequence of events fits exactly the sequence of events predicted by Vaughn (1989). As the growth cone was very dim, the contrast in these images was enhanced non linearly by adjusting the gamma to 1.5 . In the bottom sequence (lower rectangle in low magnification image) a new cluster (arrowhead) is observed to appear along the shaft of a preexisting dendrite. Note that the appearance of these clusters is not preceded by the coalescence of discrete fluorescent clusters. Bar, 5 μm. (B, C) Changes in the fluorescence of SAP90/PSD-95:GFP clusters (old and new) labeled in the rightmost panels in A. Data is not normalized or background corrected. (D) Average time course of new SAP90/PSD-95:GFP cluster formation. Data from 56 new clusters was normalized and pooled together as described in Experimental Methods. The dashed line is of a single exponential with a time constant of 23 minutes fit to the data. Note that as new clusters had formed at different time points in time lapse sessions, not all new clusters were followed for the same duration. Thus the mean and standard deviation values shown here for time points equal or greater than 120 min hours are of decreasing numbers of events that are indicated below such time points. (E) Time course of changes in the fluorescence intensity of 40 preexisting clusters. No significant changes were observed except a small gradual decrease in fluorescence intensity probably resulting from photobleaching (0.0004 normalized units per minute, linear regression, dashed line).

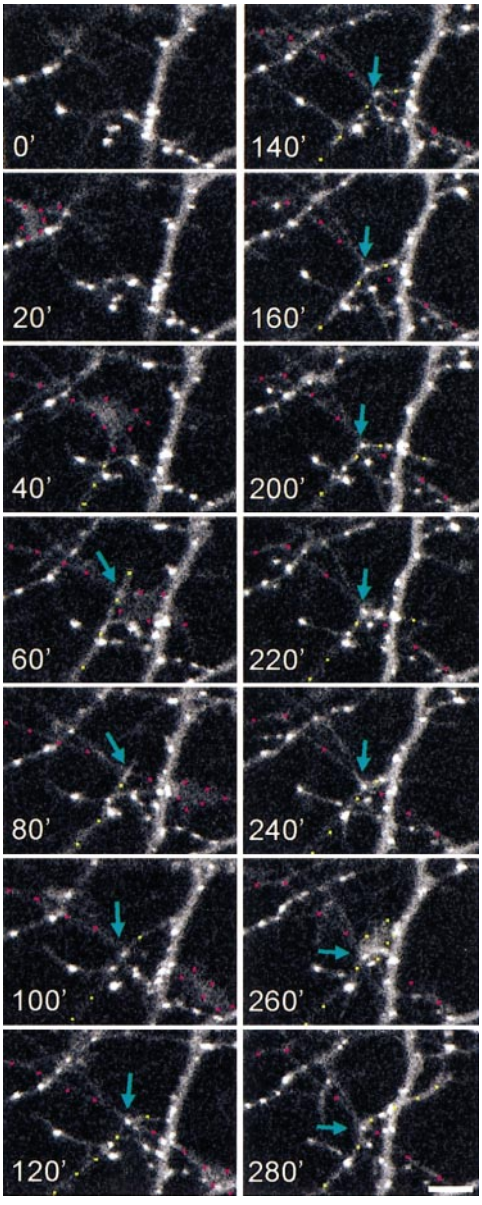

FIG. 8. Formation of a new SAP90/PSD-95:GFP cluster at the intersection of an elongating axon and an elongating dendrite. A faintly fluorescent axon, lead by a motile growth cone was observed to cross the field of view diagonally and contact an elongating dendrite (t = 60′, arrow). A new cluster of SAP90/PSD-95:GFP was observed to form at the contact site over the next 40–60 min, which persisted until the end of the time lapse session (arrows). Interestingly, the elongating dendrite seemed to stall for a while, extending and retracting filopodia, before developing a new growth cone (t = 260′) and continuing to extend (t = 280′). As the axonal fluorescence was very weak, contrast was enhanced nonlinearly by adjusting the gamma of these images to 1.2. In addition, the interacting axon and dendrite were tagged with small hand-drawn pink and yellow dots respectively. Bar, 5 μm.

found to be significantly larger (El-Husseini *et al.*, 2000). Alternatively, the numerous interactions that SAP90/PSD-95 participates in could allow it to cluster at synaptic sites via interactions with other PSD molecules, in effect bypassing the experimentally introduced perturbation. Future experiments based on strategies similar to those used here, but expanded to include the concomitant expression of additional, spectrally separable fluorescent PSD molecules such as Neuroligin, GluR1, NR1, or Stargazin should provide important information on the temporal order of synaptic assembly, and consequently, on the roles of specific PSD molecules in the assembly of the glutamatergic synapse.

EXPERIMENTAL METHODS

Cell Culture

Hippocampal cell cultures were prepared as described previously (Ryan *et al.*, 1993). Briefly hippocampal CA1–CA3 regions were dissected from 1- to 3-day-old Sprague–Dawley rats, dissociated by trypsin treatment followed by triturization with a siliconized Pasteur pipette and then plated onto coverslips coated with poly-d-lysine (Sigma, U.S.A.) inside 6- or 8-mm-diameter glass cylinders (Bellco Glass, NJ). Culture media consisted of minimal essential media (Gibco BRL, MD), 0.6% glucose, 0.1g/liter bovine transferrin (Calbiochem, CA), 0.25 g/liter insulin (Sigma), 0.3 g/liter glutamine, 5–10% FCS (Sigma), 2% B-27 supplement (Gibco), and 8 μM cytosine β-d-arabinofuranoside (Sigma). Cultures were maintained at 37°C in 95% air 5% CO_2 humidified incubator, and culture media was replaced every 3–7 days. Experiments were performed on preparations grown in culture for 8–12 days.

Cell Fractionation

Cell fractionation was performed as described previously (Zhai *et al.*, 2001). In brief, brains were dissected out and homogenized in homogenization buffer (5 mM Hepes, pH 7.4, 0.5 mM EDTA, 0.3 M sucrose, protease inhibitor cocktail). The homogenate was centrifuged at 800*g* for 20 min, and the crude membrane in the supernatant fraction was then centrifuged at 100,000*g* for 1 h. The P100 pellet was resuspended in an equal volume of homogenization buffer as the S100 supernatant before Western blotting. Alternatively, for cell fractionation, the crude membrane fraction was hypotonically lysed by adding 9 vol of H_2O and the membrane concentrated by centrifugation at 100,000*g*. The P100 or S100 fractions

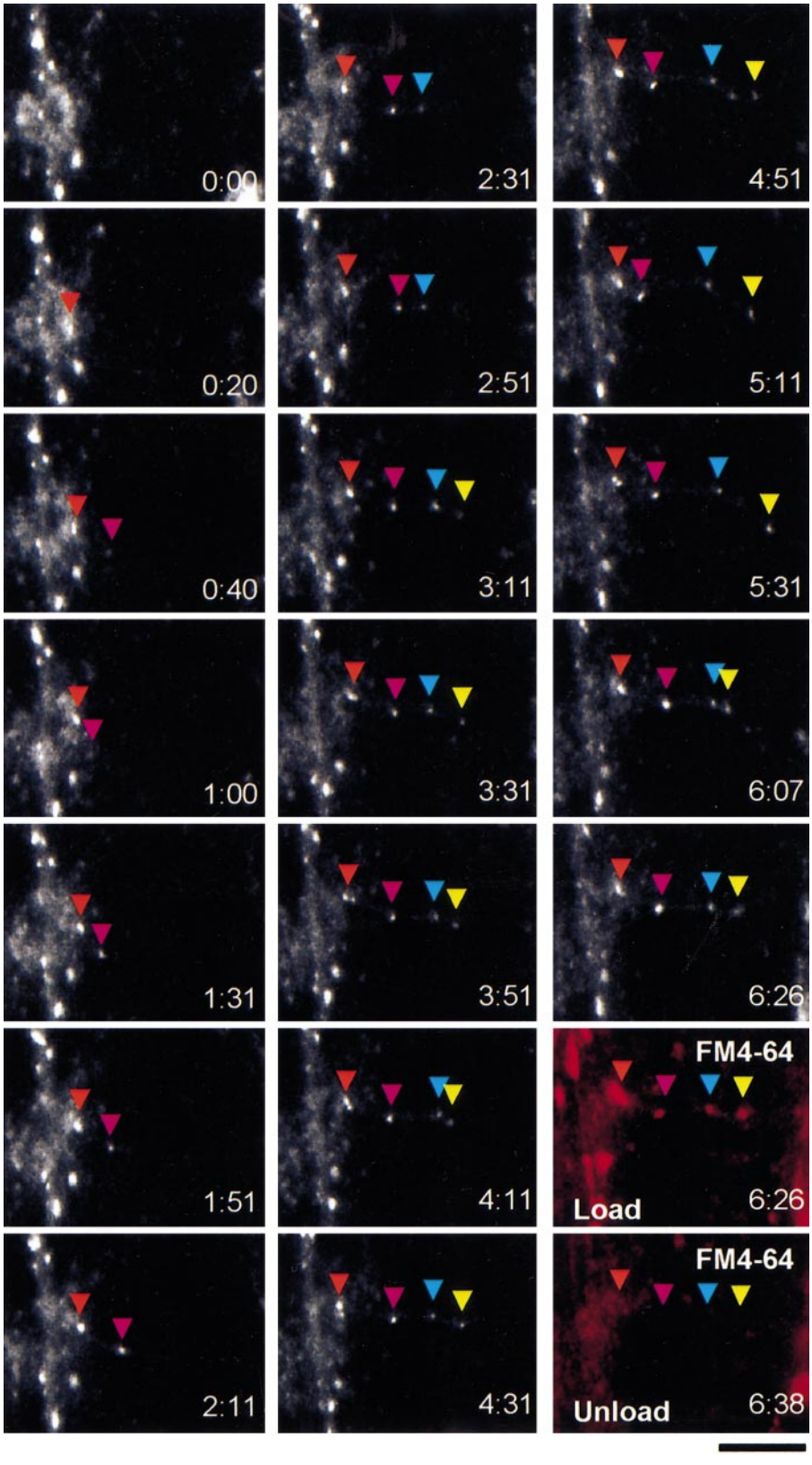

FIG. 9. New SAP90/PSD-95:GFP clusters are synaptic. A series of four new SAP90/PSD-95:GFP clusters were observed to form sequentially along an elongating dendritic branch (colored arrowheads). Upon labeling with FM 4–64, all four SAP90/PSD-95:GFP clusters were found to be associated with functional presynaptic boutons as determined by their capacity for stimulation-evoked endocytosis and exocytosis of FM 4–64. Bar, 10 μm.

were then adjusted to 2 M sucrose and loaded as a layer at the bottom of a discontinuous sucrose gradient underneath layers of 1.2, 0.8, and 0.3 M sucrose. The sucrose gradient was centrifuged at 268,000*g* for 3 h. Fractions (1.5 ml) were then taken from the top of the gradient to the bottom, separated on an 8% SDS–PAGE, transferred to Nitrocellulose and probed with antibodies against SAP90/PSD-95 (Upstate Biotechnology; Lake Placid, NY) or synaptophysin (Roche Diagnostics GmbH, Mannheim, Germany).

Expression of EGFP-Tagged Proteins in Hippocampal Neurons

SAP90/PSD-95:GFP (Arnold and Clapham, 1999) was provided as a generous gift by Dr. David Clapham of Howard Hughes Medical Institute and Children's Hospital (Boston, MA). ANP:GFP was provided as a generous gift by Dr. Edwin S. Levitan of the University of Pittsburgh. Transfection of hippocampal neurons with these plasmids was based on the calcium phosphate transfection method described by Kohrmann and coworkers (1999). Briefly, cells raised in culture for 5–7 days were washed with fresh, serum free medium (MEM + 5 g/liter glucose), after saving original media, and left in incubator for 45 min. Then 6 μl of a calcium-phosphate precipitate-DNA mixture (see below) was added to each glass cylinder, and cells were returned to an incubator with an atmospheric environment of 2.5% CO_2, 97.5% air, for 90–105 min. Cells were then washed twice with Hepes-buffered media (HBS), twice with serum-free medium, after which the original growth medium was returned to the glass cylinders. Precipitate was prepared by adding 5 μg DNA to 60 μl of 2 M $CaCl_2$, and then adding 60 μl 2× BES solution at pH 6.95, while vigorously mixing the test tube (see Kohrmann *et al.*, 1999 for HBS and BES solution formulations). Precipitate mixture was adding immediately to cloning cylinders. Transfection was evaluated after 24 h by fluorescence microscopy. Expression of exogenous DNA was typically detected in 2–10 neurons per cloning cylinder.

Microscopy

Scanning fluorescence and DIC images were acquired using a confocal laser scanning microscope designed by Drs. S. J. Smith (Stanford University School of Medicine) and T. A. Ryan (Weill Medical College of Cornell University), using a Zeiss 40× 1.3 N.A. Fluar objective. The system is controlled by software written by one of us (N.E.Z.) and includes provisions for automated, multisite time lapse microscopy (Vardinon-Friedman *et al.*, 2000; Zhai *et al.*, 2001). EGFP and FM 4–64 were excited using the 488 nm line of an argon laser. Fluorescence emissions were read using 500–545 nm band-pass and >630 nm long-pass filters, respectively (Chroma, VT). DIC images were acquired by collecting the transmitted laser light with a photomultiplier placed at the end of the Zeiss microscope DIC optical train.

Time-lapse recordings were carried out by averaging two frames collected at each of 5–7 focal planes spaced 0.8 μm apart. All data was collected at 640 × 480 resolution, at 12 bits/pixel, with the confocal aperture partially open. To increase experimental throughput, data was collected sequentially from up to 12 predefined sites, using the CLSM robotic XYZ stage to cycle automatically through these sites at predetermined time intervals. Focal drift during the experiment was corrected automatically using the CLSM "autofocus" feature developed by Dr. S. J. Smith: Each time the XYZ stage reached a predefined site, the focal plane of the medium/coverslip interface was determined automatically and image stacks were collected at predefined offsets above this plane.

In most experiments, preparations were imaged within their cloning cylinders in the presence of their growth media (no perfusion). The coverslips were mounted in a modified heated chamber (Warner Instrument Corp., CT), placed in a custom designed enclosure flooded with a sterile mixture of 5% CO_2 and 95% air. The chamber and objective were heated to 37–38°C using resistors and thermal foil and were controlled separately. This setup resulted in stable intrachamber temperatures of 37°C.

Functional Labeling of Presynaptic Boutons with FM 4–64

Functional presynaptic boutons were visualized by loading them with FM 4–64 (*N*-(3-triethylammoniumpropyl)-4-(*p*-dibutylaminostyryl)pyridinium, dibromide, Molecular Probes, OR). For these experiments the cloning cylinder was removed and cells were perfused with Tyrodes saline solution (119 mM NaCl, 2.5 mM KCl, 2 mM $CaCl_2$, 2 mM $MgCl_2$, 25 mM Hepes, 30 mM glucose, buffered to pH 7.4), to which the ionotropic glutamate receptor antagonist 6,7-dinitroquinoxaline-2,3-dione (DNQX, Research Biochemicals International, MA) was added from 2000× stocks in dimethyl sulfoxide (DMSO) to a final concentration of 10 μM. Cells were exposed to FM 4–64 by flooding the perfusion chamber with Tyrodes containing 15 μM FM 4–64 and 10 μM DNQX. The neurons were then stimulated to fire

action potentials by passing 1 ms current pulses through platinum electrodes placed on both sides of the chamber. The cells were stimulated for 30 s at 10 Hz, left in the dye for an additional 30 s, washed for 1 min with 1mM ADVASEP 7 (β-Cyclodextrin Sulfbutyl Ether, Cydex, KS) (Kay *et al.*, 1999) in Tyrodes solution containing 10 μM DNQX and rinsed with Tyrodes for 2–3 min. Dye unloading was performed by stimulating the neurons for 120 s at 10 Hz.

Retrospective Immunohistochemistry

Neurons were fixed by flooding the perfusion chamber with a fixative solution consisting of 4% formaldehyde and 120 mM sucrose in phosphate buffered saline (PBS) for 20 min. The cells were permeabilized for 10 min in fixative solution to which 0.25% Triton X-100 (Sigma) was added. The cells were washed three times in PBS, incubated in 10% bovine serum albumin (BSA) for 1 h at 37°C, and incubated overnight at 4°C or room temperature with primary antibodies in PBS and 1% BSA. The cells were then rinsed three times for 10 min with PBS and incubated for 1 h at room temperature with secondary antibodies in PBS and 1% BSA. The cells were rinsed again with PBS, mounted, and imaged immediately. In some experiments designed to examine the cytoplasmic distribution of SAP90/PSD-95, Saponin (0.025%, Sigma) was used instead of Triton X-100 for plasma membrane permeabilization.

Primary antibodies used in this study included monoclonal mouse anti-SAP90/PSD-95 (clone 7E3-1B8; Affinity Bioreagents Inc. CO, and clone K28/43; Upstate Biotechnology NY), rabbit anti-GluR1 (Chemicon International Inc., CA) and monoclonal anti MAP2 (Sigma, clone HM-2). Secondary antibodies used were Cy3 anti-rabbit (Jackson ImmunoResearch Laboratories, U.S.A.) or tetramethylrhodamine goat anti-rabbit (Molecular probes) and Cy-5 Donkey anti-mouse (Chemicon).

To facilitate the location of the same sites for which data was collected during experiments, a small cross was etched on a cell-free region of each coverslip, and coordinates of all sites were stored as offsets from this fiduciary mark to computer files. These coordinate sets were then used to locate the same sites after remounting the fixed and processed specimens on the microscope. Specimen position was then corrected manually by comparing DIC images obtained during the experiment with those of the fixed tissue, and images of immunolabeled cells were collected by averaging 4 frames at 6 sections spaced 0.5 μm apart with the confocal aperture nearly fully closed. Cy3/Tetramethylrhodamine fluorescence was recorded at 532 nm excitation (frequency doubled NdYag laser line)/>565 nm emission and Cy-5 fluorescence was recorded at 633 nm excitation (Helium-Neon 633 line)/>650 emission.

Image Analysis

All data analysis was performed using software ("OpenView") written for this purpose by one of us (N.E.Z.). Except where stated otherwise, analysis was performed on maximal intensity projections of Z section stacks. Digital movies of time lapse sequences were prepared for each site and thereafter used for evaluating the dynamics of fluorescent puncta, and for detecting new SAP90/PSD-95:GFP clusters.

Quantitative analysis of SAP90/PSD-95:GFP expression levels and there effects on GluR1 expression were performed as follows: analysis boxes were centered over fluorescent puncta in maximal intensity projection images of neurons expressing SAP90/PSD-95:GFP and of images obtained at the same regions after fixation and immunolabeling against SAP90/PSD-95 or GluR1. The average intensity of the central 3×3 pixels in each box was then determined. In each dish, immunolabeled puncta were divided into two groups according to the presence or absence of SAP90/PSD-95:GFP clusters at the same locations (presumably reflecting puncta belonging to neurons expressing SAP90/PSD-95:GFP and to naive neurons respectively), and the average fluorescence intensities of immunolabeled puncta in each group were calculated and compared. In some experiments relationships between GFP and antibody fluorescence were determined for individual, SAP90/PSD-95:GFP cluster-matched puncta. The linear relationships between the two measures revealed in Figs. 1F and 1G indicate that both measures scale linearly with the quantity of GFP-tagged and total SAP90/PSD-95, respectively, although it remains possible, if unlikely, that both measures deviate from linearity in an identical fashion.

Changes in the fluorescence intensity of new SAP90/PSD-95:GFP clusters were measured in original image sets by centering an 11×11 pixels box (about 1.5×1.5 μm) on the new cluster and measuring the average intensity in this box. These measurements were then performed in all consecutive frames. The background fluorescence was measured separately for each new cluster, by measuring the average fluorescence in the image collected just prior to the first appearance of the new cluster at the location where it appeared in the subsequent frame. All intensity measurements of all new clusters were normalized by subtracting the back-

ground intensity from all subsequent measurements, and dividing all resulting values by the (background-subtracted) peak intensity value collected for that cluster during the time lapse session. The normalized values for all new clusters were then averaged for each time point, where time 0 was considered to be the time of the frame collected just prior to the first appearance of the new cluster. Only clusters followed for at least 100 min were included in this analysis.

Fluorescence intensity measurements of preexisting clusters and normalization of this data was performed in a similar manner except that in this case, no background subtraction was performed.

Due to the tendency of many SAP90/PSD-95:PSD clusters to change their position slowly over time (as in Fig. 3), we did not include in our analysis new clusters that had formed or moved too close (<3 μm) to other SAP90/PSD-95:GFP clusters.

Quantitative assessment of association of SAP90/PSD-95:PSD clusters with FM 4–64 labeled puncta was performed as described previously (Vardinon-Friedman *et al.*, 2000), except that in this case, as fluorescence images of SAP90/PSD-95:GFP and FM 4–64 were collected concomitantly in live neurons, the criteria were more severe, and only SAP90/PSD-95:PSD clusters in direct contact with a FM 4–64 punctum were scored as clusters associated with a functional presynaptic bouton.

Figures were prepared using commercial software (Adobe Photoshop, Microsoft Excel and Microsoft PowerPoint).

ACKNOWLEDGMENTS

We are grateful to Larisa Goldfeld and Vladimir Lyakhov for their invaluable technical assistance, to Dr. David Clapham for the provision of the SAP90/PSD-95:GFP construct, to Edwin Levitan for provision of the ANP:GFP construct, and to Drs. Tim Ryan, Eckart Gundelfinger, and Thomas Dresbach for their generous assistance. This work was supported by grants from the Israel Science Foundation (139/98) to N.E.Z. and the NIH (RO1 NS39471, PO1 AG06569) to C.C.G. N.E.Z. is a member of the Bernard Katz Minerva Center for Cell Biophysics.

REFERENCES

Ahmari, S. E., Buchanan, J., and Smith, S. J. (2000). Assembly of presynaptic active zones from cytoplasmic transport packets. *Nat. Neurosci.* **3:** 445–451.

Arnold, D. B., and Clapham, D. E. (1999). Molecular determinants for subcellular localization of PSD-95 with an interacting K+ channel. *Neuron* **23:** 149–157.

Burke, N. V., Han, W., Li, D., Takimoto, K., Watkins, S. C., and Levitan, E. S. (1997). Neuronal peptide release is limited by secretory granule mobility. *Neuron* **19:** 1095–1102.

Burns, M. E., and Augustine, G. J. (1995). Synaptic structure and function: Dynamic organization yields architectural precision. *Cell* **83:** 187–194.

Caceres, A., Banker, G., Steward, O., Binder, L., and Payne, M. (1984). MAP2 is localized to the dendrites of hippocampal neurons which develop in culture. *Brain Res.* **315:** 314–318.

Cantallops, I., and Cline, H. T. (2000). Synapse formation: If it looks like a duck and quacks like a duck. . . . *Curr. Biol.* **10:** R620–R623.

Chen, L., Chetkovich, D. M., Petralia, R. S., Sweeney, N. T., Kawasaki, Y., Wenthold, R. J., Bredt, D. S., and Nicoll, R. A. (2000). Stargazin regulates synaptic targeting of AMPA receptors by two distinct mechanisms. *Nature* **408:** 936–943.

Cho, K. O., Hunt, C. A., and Kennedy, M. B. (1992). The rat brain postsynaptic density fraction contains a homolog of the Drosophila discs-large tumor suppressor protein. *Neuron* **9:** 929–942.

Cochilla, A. J., Angleson, J. K., and Betz, W. J. (1999). Monitoring secretory membrane with FM1–43 fluorescence. *Annu. Rev. Neurosci.* **22:** 1–10.

Craig, A. M., Blackstone, C. D., Huganir, R. L., and Banker, G. (1993). The distribution of glutamate receptors in cultured rat hippocampal neurons: Postsynaptic clustering of AMPA-selective subunits. *Neuron* **10:** 1055–1068.

Craven, S. E., El-Husseini, A. E., and Bredt, D. S. (1999). Synaptic targeting of the postsynaptic density protein PSD-95 mediated by lipid and protein motifs. *Neuron* **22:** 497–509.

Dresbach, T., Qualmann, B., Kessels, M., Garner, C. C., and Gundelfinger, E. D. (2001). The presynaptic cytomatrix of brain synapses. *Cell. Mol. Life. Sci.* **58:** 94–116.

El-Husseini, A. E., Craven, S. E., Chetkovich, D. M., Firestein, B. L., Schnell, E., Aoki, C., and Bredt, D. S. (2000a). Dual palmitoylation of PSD-95 mediates its vesiculotubular sorting, postsynaptic targeting, and ion channel clustering. *J. Cell Biol.* **148:** 159–172.

El-Husseini, A. E., Schnell, E., Chetkovich, D. M., Nicoll, R. A., and Bredt, D. S. (2000b). PSD-95 involvement in maturation of excitatory synapses. *Science* **290:** 1364–1368.

Garner, C. C., Kindler, S., and Gundelfinger, E. M. (2000a). Molecular determinants of presynaptic active zones. *Curr. Opin. Neurobiol.* **10:** 321–327.

Garner, C. C., Nash, J., and Huganir, R. L. (2000b). PDZ proteins in synapse assembly and signaling. *Trends Cell Biol.* **10:** 274–280.

Goldstein, L. S., and Yang, Z. (2000). Microtubule-based transport systems in neurons: The roles of kinesins and dyneins. *Annu. Rev. Neurosci.* **23:** 39–71.

Han, W., Li, D., Stout, A. K., Takimoto, K., and Levitan, E. S. (1999). Ca2+-induced deprotonation of peptide hormones inside secretory vesicles in preparation for release. *J. Neurosci.* **19:** 900–905.

Harlow, M. L, Ress, D., Stoschek, A., Marshall, R. M., and Mcmahan, U. J. (2001). The architecture of active zone material at the frog's neuromuscular junction. *Nature* **409:** 479–484.

Hille-Rehfeld, A. (1995). Mannose 6-phosphate receptors in sorting and transport of lysosomal enzymes. *Biochim. Biophys. Acta* **1241:** 177–194.

Husi, H., Ward, M. A., Choudhary, J. S., Blackstock, W. P., and Grant, S. G. (2000). Proteomic analysis of NMDA receptor-adhesion protein signaling complexes. *Nat. Neurosci.* **3:** 661–669.

Irie, M., Hata, Y., Takeuchi, M., Ichtchenko, K., Toyoda, A., Hirao, K., Takai, Y., Rosahl, T. W., and Sudhof, T. C. (1997). Binding of neuroligins to PSD-95. *Science* **277:** 1511–1515.

Jontes, J. D., Buchanan, J., and Smith, S. J. (2000). Growth cone and

dendrite dynamics in zebrafish embryos: Early events in synaptogenesis imaged *in vivo. Nat. Neurosci.* **3:** 231–237.

Kay, A. R., Alfonso, A., Alford, S., Cline, H. T., Holgado, A. M., Sakmann, B., Snitsarev, V. A., Stricker, T. P., Takahashi, M., and Wu, L. G. (1999). Imaging synaptic activity in intact brain and slices with FM1–43 in C. elegans, lamprey, and rat. *Neuron* **24:** 809–817.

Kennedy, M. B. (2000). Signal-processing machines at the postsynaptic density. *Science* **290:** 750–754.

Kim, J. H., and Huganir, R. L. (1999). Organization and regulation of proteins at synapses. *Curr. Opin. Cell Biol.* **11:** 248–254.

Kistner, U., Wenzel, B. M., Veh, R. W., Cases-Langhoff, C., Garner, A. M., Appeltauer, U., Voss, B., Gundelfinger, E. D., and Garner, C. C. (1993). SAP90, a rat presynaptic protein related to the product of the Drosophila tumor suppressor gene dlg-A. *J. Biol. Chem.* **268:** 4580–4583.

Kohrmann, M., Haubensak, W., Hemraj, I., Kaether, C., Lessmann, V. J., and Kiebler, M. A. (1999). Fast, convenient, and effective method to transiently transfect primary hippocampal neurons. *J. Neurosci. Res.* **58:** 831–835.

Lahey, T., Gorczyca, M., Jia, X. X., and Budnik, V. (1994). The Drosophila tumor suppressor gene dlg is required for normal synaptic bouton structure. *Neuron* **13:** 823–835.

Mammen, A. L., Huganir, R. L., and O'Brien, R. J. (1997). Redistribution and stabilization of cell surface glutamate receptors during synapse formation. *J. Neurosci.* **17:** 7351–7358.

Migaud, M., Charlesworth, P., Dempster, M., Webster, L. C., Watabe, A. M., Makhinson, M., He, Y., Ramsay, M. F., Morris, R. G., Morrison, J. H., O'Dell, T. J., and Grant, S. G. (1998). Enhanced long-term potentiation and impaired learning in mice with mutant postsynaptic density-95 protein. *Nature* **396:** 433–439.

Missler, M., and Sudhof, T. H. (1998). Neurexins: Three genes and 1001 products. *Trends Genet.* **14:** 20–26.

O'Brien, R. J., Mammen, A. L., Blackshaw, S., Ehlers, M. D., Rothstein, J. D., and Huganir, R. L. (1997). The development of excitatory synapses in cultured spinal neurons. *J. Neurosci.* **17:** 7339–7350.

Okabe, S., Kim, H. D., Miwa, A., Kuriu, T., and Okado, H. (1999). Continual remodeling of postsynaptic density and its regulation by synaptic activity. *Nat. Neurosci.* **2:** 804–811.

Passafaro, M., Sala, C., Niethammer, M., and Sheng, M. (1999). Microtubule binding by CRIPT and its potential role in the synaptic clustering of PSD-95. *Nat. Neurosci.* **2:** 1063–1069.

Rao, A., and Craig, A. M. (1997). Activity regulates the synaptic localization of the NMDA receptor in hippocampal neurons. *Neuron* **19:** 801–812.

Rao, A., Kim, E., Sheng, M., and Craig, A. M. (1998). Heterogeneity in the molecular composition of excitatory postsynaptic sites during development of hippocampal neurons in culture. *J. Neurosci.* **18:** 1217–1229.

Roos, J., and Kelly, R. B. (2000). Preassembly and transport of nerve terminals: A new concept of axonal transport. *Nat. Neurosci.* **3:** 415–417.

Ryan, T. A., Reuter, H., Wendland, B., Schweizer, F. E., Tsien, R. W., and Smith, S. J. (1993). The kinetics of synaptic vesicle recycling measured at single presynaptic boutons. *Neuron* **11:** 713–724.

Scheiffele, P., Fan, J., Choih, J., Fetter, R., and Serafini, T. (2000). Neuroligin expressed in nonneuronal cells triggers presynaptic development in contacting axons. *Cell* **101:** 657–669.

Setou, M., Nakagawa, T., Seog, D. H., and Hirokawa, N. (2000). Kinesin superfamily motor protein KIF17 and mLin-10 in NMDA receptor-containing vesicle transport. *Science* **288:** 1796–1802.

Sheng, M., and Lee, S. H. (2000). Growth of the NMDA receptor industrial complex. *Nat. Neurosci.* **3:** 633–635.

Sheng, M., and Pak, D. T. (1999). Glutamate receptor anchoring proteins and the molecular organization of excitatory synapses. *Ann. N.Y. Acad. Sci.* **868:** 483–493.

Shi, S. H., Hayashi, Y., Petralia, R. S., Zaman, S. H., Wenthold, R. J., Svoboda, K., and Malinow, R. (1999). Rapid spine delivery and redistribution of AMPA receptors after synaptic NMDA receptor activation. *Science* **284:** 1811–1816.

Vaughn, J. E. (1989). Fine structure of synaptogenesis in the vertebrate central nervous system. *Synapse* **3:** 255–285.

Vardinon-Friedman, H., Bresler, T., Garner, C. C., and Ziv, N. E. (2000). Assembly of new individual excitatory synapses—Time course and temporal order of synaptic molecule recruitment. *Neuron* **27:** 57–79.

Walikonis, R. S., Jensen, O. N., Mann, M., Provance, D. W., Jr., Mercer, J. A., and Kennedy, M. B. (2000). Identification of proteins in the postsynaptic density fraction by mass spectrometry. *J. Neurosci.* **20:** 4069–4080.

Zhai, R., Vardinon Friedman, H., Cases-Langhoff, C., Becker, B., Eckart, D., Gundelfinger, E. D., Ziv, N. E., and Garner, C. C. (2001). Assembling the presynaptic active zone: Characterization of an active zone precursor vesicle. *Neuron* **29:** 131–143.

Received April 10, 2001
Revised May 29, 2001
Accepted June 6, 2001